PROCEEDINGS OF SPIE

SPIEDigitalLibrary.org/conference-proceedings-of-spie

Stray light analysis and reduction for IFU spectrograph LLAMAS

Frostig, Danielle, Piotrowski, John, Clark, Kristin, Coppeta, David, Egan, Mark, et al.

Danielle Frostig, John Piotrowski, Kristin Clark, David Coppeta, Mark Egan, Gábor Fűrész, Michelle Gabutti, Rebecca Masterson, Andrew Malonis, Robert A. Simcoe, "Stray light analysis and reduction for IFU spectrograph LLAMAS," Proc. SPIE 11447, Ground-based and Airborne Instrumentation for Astronomy VIII, 114476E (13 December 2020); doi: 10.1117/12.2562999



Event: SPIE Astronomical Telescopes + Instrumentation, 2020, Online Only

Stray Light Analysis and Reduction for IFU Spectrograph LLAMAS

Danielle Frostig^{a,b}, John Piotrowski^c, Kristin Clark^c, David Copetta^c, Mark Egan^b, Gábor Fűrész^b, Michelle Gabutti^b, Rebecca Masterson^b, Andrew Malonis^b, and Robert A. Simcoe^b

^aMIT Department of Physics, 77 Massachusetts Ave., Cambridge, MA 02139, USA ^bMIT-Kavli Institute for Astrophysics, 77 Massachusetts Ave., Cambridge, MA, USA ^cMIT Lincoln Laboratory, 244 Wood Street, Lexington, MA, USA 02420

ABSTRACT

The Large Lenslet Array Magellan Spectrograph (LLAMAS) is an Integral Field Unit (IFU) spectrograph under construction as a facility instrument for the 6.5-meter Magellan Telescopes. For each pointing, LLAMAS delivers 2400 optical spectra (λ =350-970nm) over a 37"x37" celestial solid angle with a resolution of 2000 through a densely packed microlens+fiber array and replicated low-cost spectrographs. One of our main science goals is to study circumgalactic gas through Ly α emission. To achieve the required signal-to-noise ratio for these observations, LLAMAS must minimize stray light reaching the detector: diffuse scattered light must stay below 0.25% of sky flux and ghost images must not exceed 0.1% of the source signal.

We present a non-sequential ray tracing analysis of a simplified LLAMAS model using Photon Engineering's FRED Optical Engineering Software. We focus on stray light resulting from the volume phase holographic grating and from focal ratio degradation of the fibers. The analysis feeds into a discussion of the design and fabrication of baffles to mask the primary sources of stray light. Additionally, we develop a backup system of mounting rings inside of the cameras where pre-made baffles can be quickly added as needed. Finally, we report on the laboratory performance of a 2-camera LLAMAS prototype featuring the aforementioned stray light interventions.

Keywords: Integral Field Unit Spectrograph, Stray Light, Circumgalactic Medium

1. INTRODUCTION

The Large Lenslet Array Magellan Spectrograph (LLAMAS) is a facility instrument planned for the 6.5-meter Magellan Telescopes. LLAMAS is an Integral Field Unit (IFU) spectrograph that produces a 3D data cube: at each pointing, LLAMAS records optical spectra ($\lambda=350$ -970nm) for thousands of positions across a 37"x37" solid angle on the sky. The field is split by a microlens array and sent into 2400 fibers which are then grouped into bundles and sent to eight replicated spectrographs. On each spectrograph, the beams from the 300 fibers are split by two dichroic filters into blue ($\lambda=350$ -480nm), green ($\lambda=480$ -690nm), and red ($\lambda=690$ -970nm) cameras to achieve a resolution of R=2000 across the optical bandpass (Fig. 1). This paper is part of a series of papers describing LLAMAS, including a project overview (Ref. 1) and a detailed description of the optical design (Ref. 2).

IFU spectrographs reduce acquisition and overhead time by imaging many targets at once. In one exposure, LLAMAS can compare a transient spectra to its host galaxy, or map the redshifts and dispersion velocities of many galaxies in a high-redshift galaxy cluster. Of particular interest to this paper is the study of the circumgalactic medium (CGM). At high redshifts, the CGM is easiest to study in galaxy systems near a bright background quasar that probes the gas between the galaxies. LLAMAS will simultaneously study the galaxies and quasars in these systems through Ly α emission at z > 2 and [OIII] and [OII] emission for 1.5 > z > 0. To effectively research the faint, diffuse CGM, we must reduce any unwanted stray light in the system obscuring the dim signals.

Further author information: Send correspondence to D. Frostig at frostig@mit.edu.

Ground-based and Airborne Instrumentation for Astronomy VIII, edited by Christopher J. Evans, Julia J. Bryant, Kentaro Motohara, Proc. of SPIE Vol. 11447, 114476E ⋅ © 2020 SPIE ⋅ CCC code: 0277-786X/20/\$21 ⋅ doi: 10.1117/12.2562999

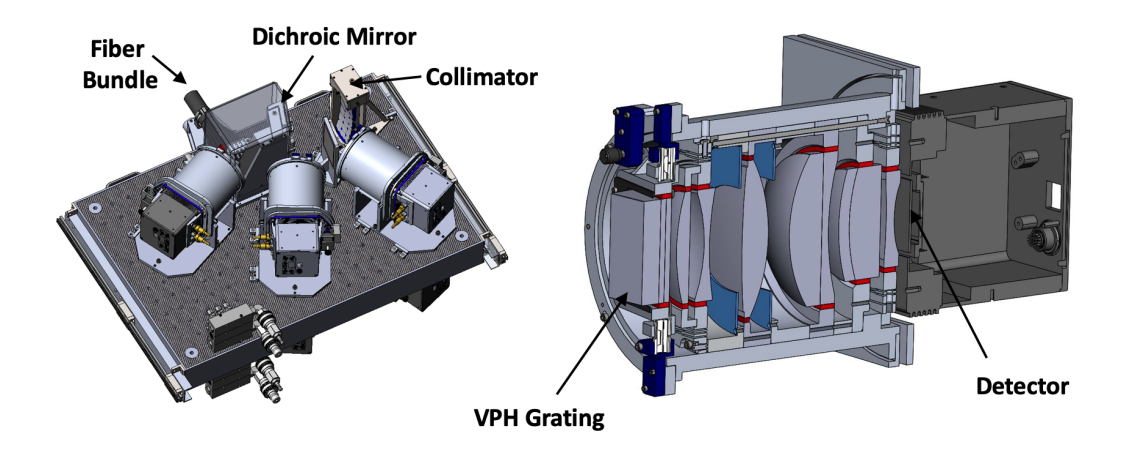


Figure 1: Overview of the LLAMAS spectrograph design. Left: One of eight spectrograph optical benches with an equivalent spectrograph on the underside of the bench. Light enters the system via a fiber bundle, is collimated at the collimator and then diverted to red, green, and blue cameras by two dichroic mirrors. Right: A cross-section of the blue camera. Light from the 300 fibers is dispersed into spectra by the virtual phase holographic (VPH) grating. Lenses and camera mechanics are shown in light gray, the RTV bonding the lenses is shown in red, baffles are shown in light blue, and the detector housing in shown in dark gray.

Broadly, stray light is any light reaching the detector that is not the primary path of light from the science target. Stray light can originate from a bright, nearby source that is not the science target-e.g. the Moon-or light from the science target taking unintended paths through the instrument. Light often reflects and scatters off of optical and mechanical surfaces diverging from the nominal optical design. When this light reaches the detector it can increase the background noise, decrease measurement fidelity, and create erroneous signals. There are two broad categories of stray light: *ghost images* from reflections off of optical elements and scattered light due to scattering off of any element in the system. There are many ways to mitigate stray light, including reducing mechanical reflectivity, improving optical coatings, and adding baffles in the path of unwanted light.

To study the CGM, LLAMAS shall detect emitting sources with surface brightness $3\times 10^{19}\frac{ergs}{cm^2sAfiber}$ at signal to noise ratio of 5 in one night of observations. In order to meet this requirement, diffuse stray light on the detector must stay below 0.25% of sky flux and concentrated stray light images must not exceed 0.1%

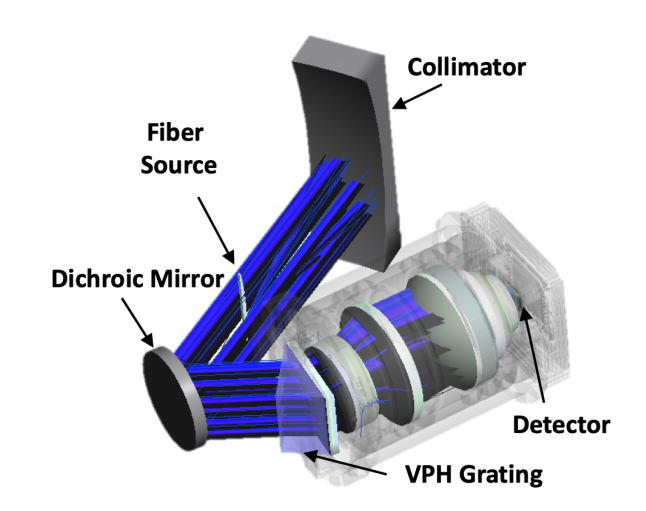


Figure 2: Simplified LLAMAS optical bench model in FRED. The light path for one fiber is shown with blue and black ray bundles traced from the fiber source to the detector.

of the source signal. We conducted a stray light analysis for LLAMAS and developed multiple mitigation strategies to satisfy these requirements.

This paper covers the creation of a simplified stray light model of LLAMAS, an outline of the non-sequential ray tracing analysis, the design of baffles and other stray light reduction strategies, and the results of laboratory testing.

2. STRAY LIGHT MODEL

The basic components of a stray light model are the light source, the optics and mechanics the rays may encounter, and a detector. The analysis consists of tracing rays from the light source and examining the ray paths that unexpectedly reach the detector. In Section 3, we will outline a non-sequential ray tracing analysis. In contrast to sequential ray tracing, in which rays hit surfaces in a predefined sequence, in *non-sequential ray tracing* rays may encounter surfaces in any order at any frequency. Non-sequential ray tracing is well suited for stray light analysis, where by definition the rays are not following the nominal light path, but can quickly become prohibitively computationally expensive as the complexity of the stray light model increases.

The LLAMAS stray light model (Figure 2) consists of one camera, the dichroic mirror, and the collimator, representing the key elements of the full spectrograph optical bench as seen in Figure 1. Of the three color channels, the blue camera ($\lambda = 350\text{-}480\text{nm}$) has the lowest instrument efficiency and light scatters more at shorter wavelengths. In this analysis, we model only the most sensitive, blue camera and apply any resultant stray light mitigation techniques to all three cameras.

2.1 Fiber source model

Light enters the spectrograph via three hundred fibers stacked vertically in a groove down the middle of the dichroic mirror. For the blue camera, each fiber emits between 350 and 480 nanometers with the weight of each wavelength scaled to match the intensity of the sky background at Las Campnanas Observatory.

The focal ratio of the fused silica fibers degrade via focal ratio degradation (FRD)—the effect whereby an input cone of light widens at the output of the fiber, leading to a faster f-number. The FRD of the LLAMAS fibers is accounted for in the optical design. The input F/4.4 cone degrades such that 95.6% of the output light falls in to the required F/4 cone of the collimator (Figure 3). The remaining 4.4% of light emitting at wider angles is by definition not on the nominal light path and is a prime source for stray light. We model the focal ratio degradation of each fiber as a non-uniform apodization sampled as a function of spherical angles matching the experimentally measured FRD shown in Figure 3.

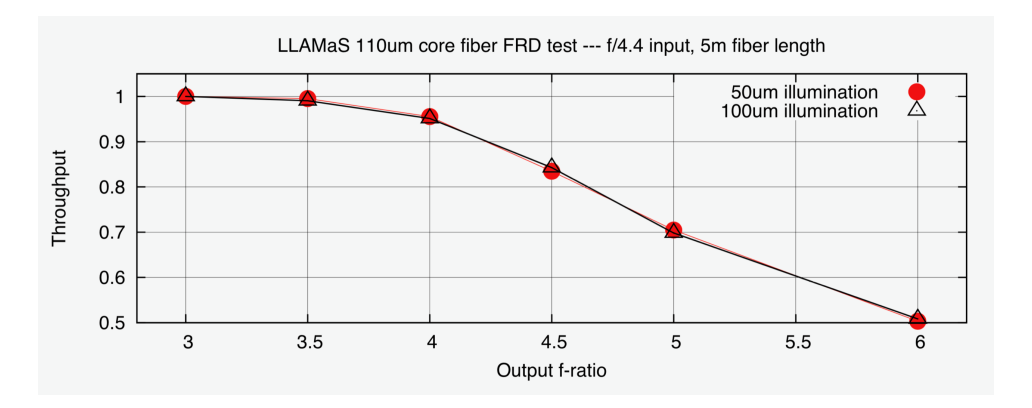


Figure 3: Focal ratio degradation of fifty cleaved optical fibers. For an input F/4.4 cone, 95.6% of the output rays subtend an F/4 cone. The result is insensitive to input illumination diameter, as shown by the convergence of the 50 micron and 100 micron samples.

2.2 Optical and Mechanical Model

We model the scattering properties of all surfaces as bidirectional scatter distribution functions (BSDF), which parameterize scattering as function of incident angle and surface properties.³

For the mechanics, we model the BSDF as a function of Lambert's cosine law. A fully Lamertian surface radiates isotropically. The aluminum surfaces that comprise the majority of the camera's mechanics are defined as half Lambertian surface and half uncoated specular reflecting surface. A half Lambertian model entails half of the incident ray power is directed into a diffuse reflection and half is a specular reflection. We similarly

assign any surfaces with unknown properties partially scattering and partially reflective attributes, to allow for the discovery of both specular and scatter stray light issues during analysis. We model the gold surfaces in the detector housing as uncoated specular reflecting surfaces, where uncoated materials abide by the Fresnel equations.

We estimate scatter from the optical surfaces with a Harvey-Shack BDSF model, as an approximation for polished surfaces such as lenses and mirrors.⁴ Additionally, we simulate all optics with anti-reflection coatings based on measured laboratory data of the as-built coatings.

2.3 Detector Model

The CCD detector model consists of three layers closely packed together to account for various interactions with light (Figure 4). First, the anti-reflection coating models how much light is transmitted or reflected, the quantum efficiency layer transmits a certain portion of photons as counts to be measured, which are then collected by the ideal detector. The high resolution of the LLAMAS detectors (2048 \times 2048 pixels) could not feasibly be modeled across the entire detector, so analyses with the full detector have a 2-by-2 pixel binning and alignment and image quality checks are preformed with 100×100 pixel detector at full resolution.

2.4 Spectrograph Bench Model

The majority of stray light is predicted to originate within the camera. Consequently, spectrograph bench model only includes key optics predicted to contribute to stray light: the collimator and one dichroic mirror (Figure 2). Light travels from the fibers in the middle of the dichroic mirror, to the collimator, back to the dichroic mirror to be split into the blue wavelengths, and into the camera via the VPH grating. The preexisting design of dichroic and collimator housing features baffling around the optics anodized with black paint. The model represents the two baffles as black Lambertian surfaces.

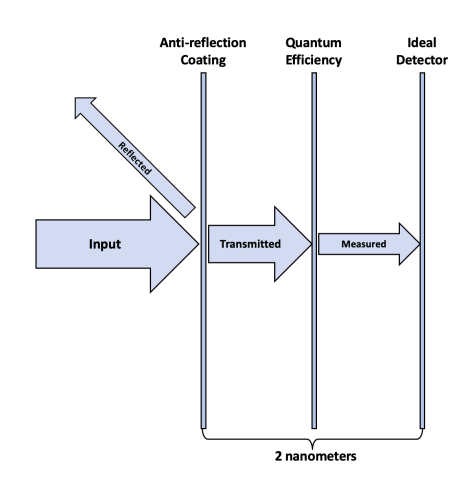


Figure 4: A model of the detector employed to account for reflections and quantum efficiency losses in the proper order. The three layers are packed in tightly to simulate one continual surface.

3. STRAY LIGHT ANALYSIS

Analyzing stray light within the spectrograph bench model involves a series of raytraces to search for problematic light paths. Once these paths are identified, the highest power paths are better characterized by retracing sequentially with a much larger quantity of rays. From the sequential traces we are able to extract high fidelity results for ray path power, peak irradiance, and the spatial extent on the focal plane. After characterization we determine whether a given path falls within our system requirements. If a path does not, then actions are taken to mitigate the amount of stray light reaching the focal plane.

3.1 Model Validation

Model agreement is done visually and analytically. Visually we ensure that the optics and mechanics are well-aligned and that rays are tracing to their correct geometric location on the focal plane. Analytically we select a sample of spots across the field and compare the geometric spot size of the optomechanical FRED model with that of the optical Zemax model. Once the models yield similar spot sizes, they are considered to be in agreement.

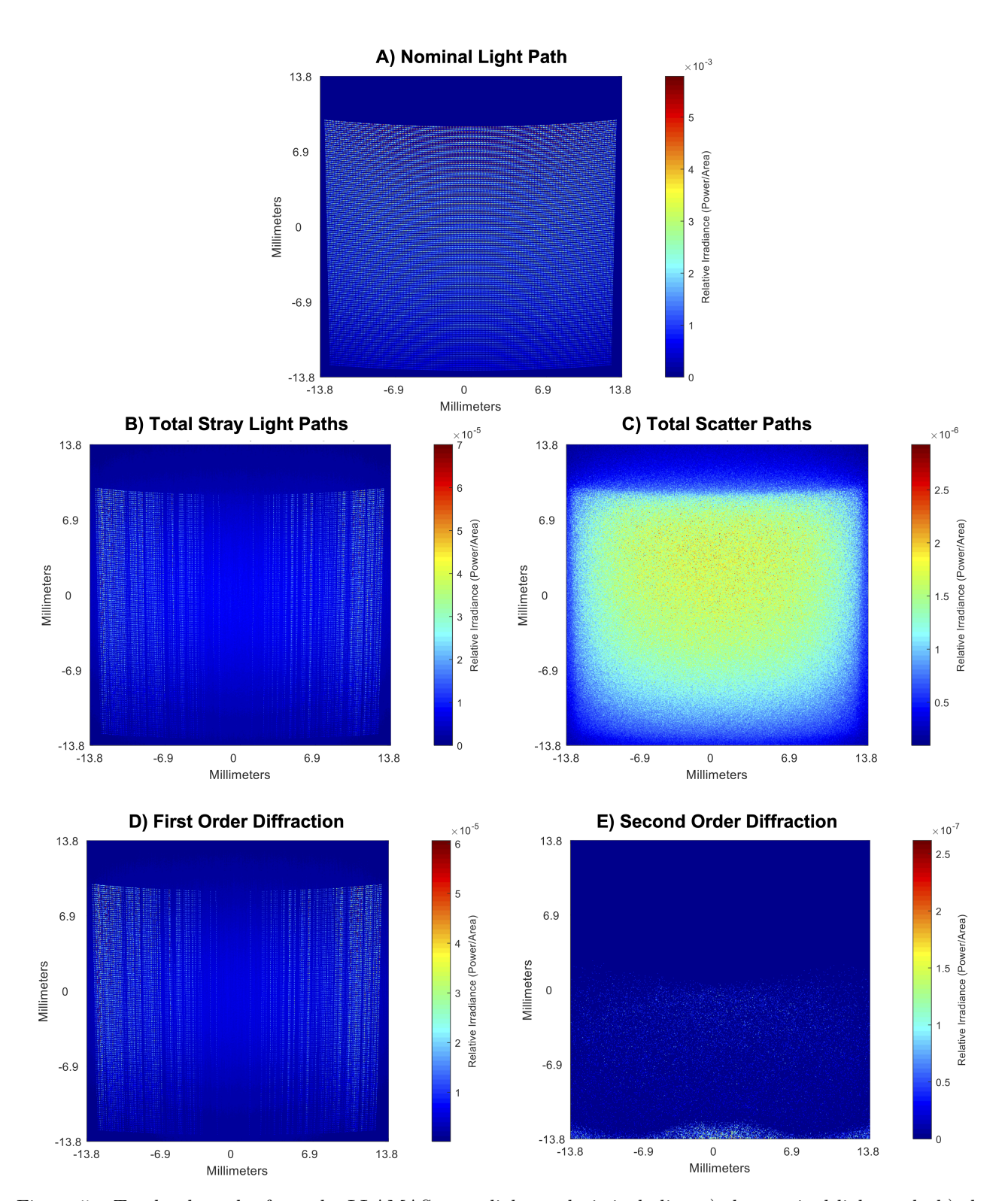


Figure 5: Top level results from the LLAMAS stray light analysis including a) the nominal light path, b) the total stray light paths, c) total scatter paths, d) first order diffraction, and e) second order diffraction. The color scale reflects relative irradiance on the detector and the scale varies for each image to more clearly demonstrate the different patterns of stray light.

3.2 Methodology

Stray light paths are any paths of light which do not follow the nominal light path. Ray paths are made up of a sequential series of element interactions; where elements can be optical or mechanical, and interactions can be specular transmission or reflections, scatter transmission or reflection, diffraction, or absorption. To find the most likely combinations of these element interactions, we perform a non-sequential ray trace. Populating a selection of the fibers with randomly sampled rays over an aperture apodized according to the FRD provides a good way of probing the system for stray light paths.

Each ray defined at the fiber array splits at each surface interaction into a set of rays, as long as the rays are above a set power threshold. For example, a ray which hits the front surface of a lens can split into a transmitted and reflected specular component, as well as scattering components. These interactions are not predetermined, so running a non-sequential trace will generate numerous unique light paths. These paths are then downselected by only considering stray light paths which put power on the focal plane.

The light paths identified from the non-sequential trace are characterized by populating the rest of the fibers and increasing the number of rays at each fiber. Increasing the ray count and tracing the light paths is done efficiently by sequential tracing because we are using the light paths previously determined by the non-sequential search. When these traces are summed together, it creates a more holistic model of the predominant causes of stray light within the spectrograph bench model.

To increase our efficiency and decrease our computation time, higher power paths are prioritized for sequential tracing. This is done because high power paths are the most likely to cause issues within the system and are the first candidates for mitigation through coating, baffling, or other techniques. Due to this bias of characterizing high power paths, this leads to an underestimate for the integrated power on the focal plane from all sources of stray light. Large quantities of low power paths, such as forward scatter paths, are under represented using this method.

3.3 Results

After filtering out the nominal signal, the remaining light paths are stray light paths. These paths can be broken down into three primary categories for LLAMAS: specular paths, scatter paths, and second-order diffraction paths. The power of the specular paths combine to 0.453% of the nominal signal, contributing to most of the stray light within the spectrograph. The highest power of these paths resulted from a reflection off the substrate of the virtual phase holographic (VPH) grating. By analyzing the spatial extent of the path, we are able to design a baffle for the camera and reduce the total stray light in the system to 0.346% of the nominal signal. This process is discussed in section 4.

The scattered light makes up the next largest portion of the stray light at 0.212% of the nominal signal. This value is most likely to be underestimated due to a bias in ray paths for higher power paths. While any given scattered path tends to have low power, there are a large number of paths which sum to a measurable quantity.

Finally there are paths from second order diffraction at the VPH grating. The steep angle of the diffracted rays and the low efficiency of the VPH in the second order resulted in the lowest combined path power of 0.0002% of the nominal signal.

4. STRAY LIGHT MITIGATION

While stray light can never be completely eliminated, it can be reduced through various techniques including careful optical design, changing surface properties in the system, and baffling unwanted paths.

4.1 VPH Grating Baffle

Light enters the camera through a virtual phase holographic (VPH) grating which disperses the light from each fiber into a spectrum from 350 to 480 nanometers. If the light from each fiber is modeled as an F/4 cone, there are no significant stray light paths from the VPH grating. However, due to the focal ratio degradation of each fiber described in section 2.1, light outside of the nominal F/4 cone reflects off of the edge of the VPH grating and creates a significant stray light path (Figure 6). The total intensity of this specular reflection is about 0.1%

of the total power on the detector. To eliminate this stray light path, we design a baffle for the inner face of the VPH grating with a 0.8mm overlap from the edge of the grating. The baffle eliminates 100% of the ghost path and leads to a 0.00% primary signal loss when modeled without focal degradation and a 0.27% primary signal loss when modeled with focal ratio degradation. The VPH baffle and the baffles described in the section below are made of Aeroglaze painted black aluminum.

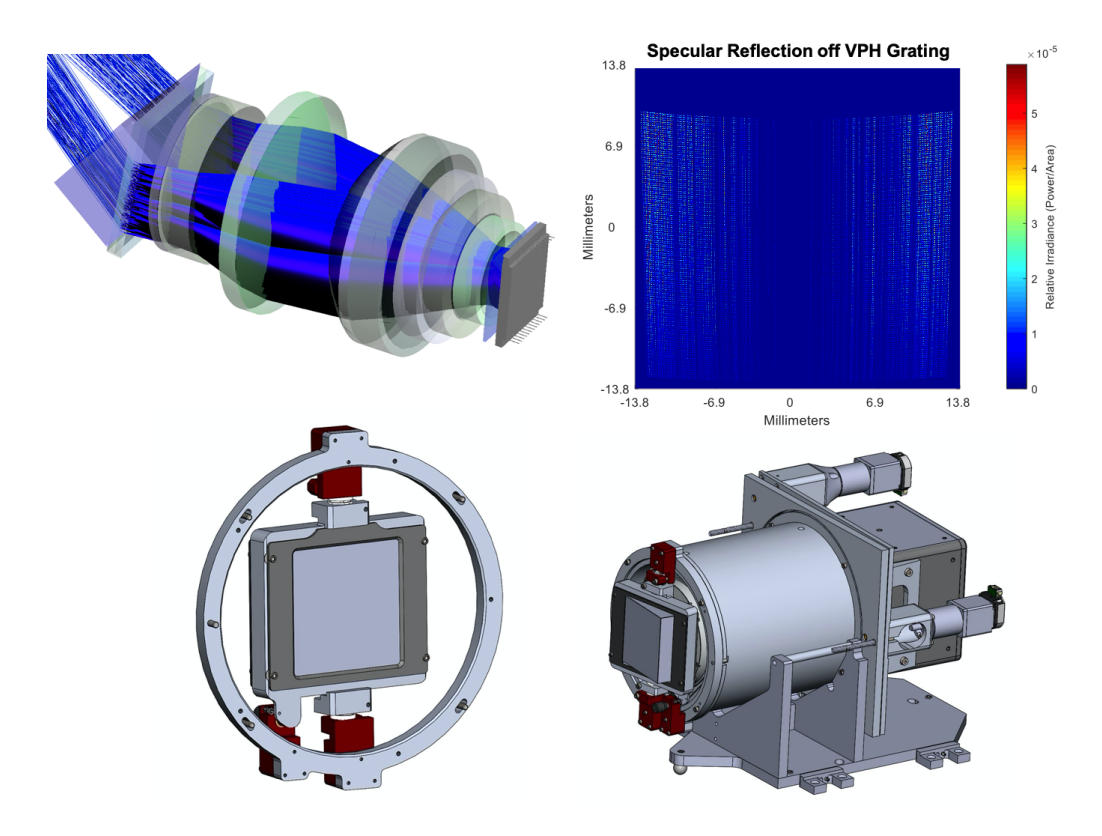


Figure 6: A stray light path reflecting off the sides of the VPH grating (upper left) produces a ghost image of approximately 0.1% of the total power on the detector (upper right). The baffle shown in dark gray (lower left) eliminates this path and is integrated into the camera housing (lower right).

4.2 Supplemental Baffles

In addition to baffling well-modeled, strong sources of stray light, we create a baffle system to block unanticipated sources of stray light. Stray light is often higher in the built instrument than models of the instrument, due to simplifications in the model and weak paths below the analysis cutoff. In anticipation of this possibility, there are two mounting rings in each camera barrel to support optional baffles. The cutout at the center of each baffle matches the footprint of the nominal light path from the shortest to longest wavelengths (Figure 7). While some stray light can still reach the detector through the cutout, the baffles block light traveling at a high angle of incidence to the detector.

5. LABORATORY VERIFICATION

To mitigate risk for the large scale IFU spectrograph, we create a prototype LLAMAS spectrograph with two cameras (see Ref. 1 for a detailed overview). Figure 8 shows an image taken of a calibration source with the blue camera on the prototype. We use a masked image with half of the fibers illuminated to estimate stray light from the inter-trace residuals. Approximately 2% of the signal is associated with stray light and the pattern of stray light increasing towards the center is consistent with scattering near the image plane and not from the

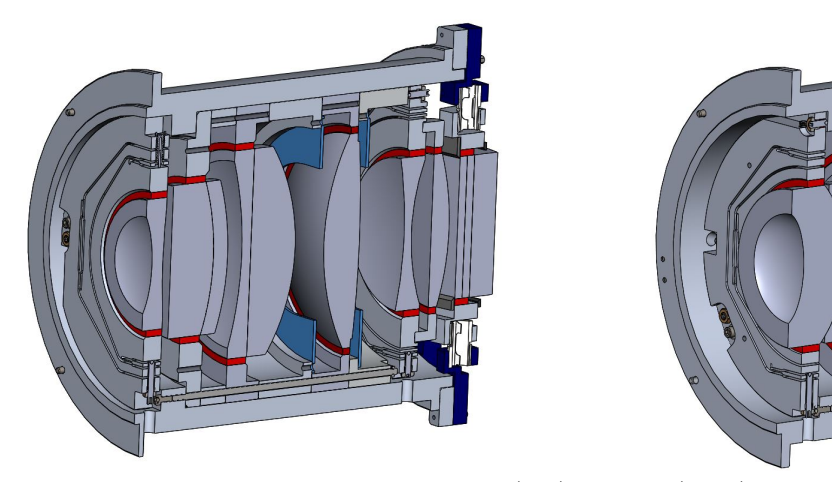


Figure 7: A backup baffle system for blue (left) and red (right) channel cameras. The baffles are shown in light blue and are differently sized to account for the respective nominal light path in each camera.

VPH grating. The stray light in the laboratory tests is higher than the modeled stray light due to the sum of many lower power paths not modeled in the analysis and because of differences in the prototype instrument and the modeled full-build instrument. For example, the prototype instrument has looser AR coating specifications and a manufacturing problem with the VPH AR coating. The stray light is modeled and subtracted from the science images as part of the prototype data reduction pipeline to meet the stray light requirements.

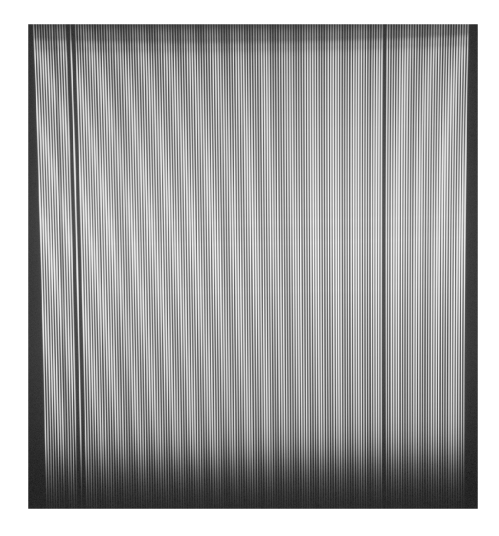


Figure 8: An image taken with the blue camera on the LLAMAS prototype in the laboratory, shown with logarithmic scaling.

6. SUMMARY

We create a non-sequential stray light model for the IFU spectrograph LLAMAS using Photon Engineering's FRED software. Results from the stray light analysis led to baffling of the VPH grating and creating a system of back-up baffles to mitigate stray light. We use laboratory images taken with the LLAMAS prototype to model stray light and subtract the stray light contribution from the science images. By reducing stray light contributions, we meet our requirements to study faint signals from the circumgalactic medium.

ACKNOWLEDGMENTS

LLAMAS is supported by the National Science Foundation under MSIP grant number 1836002 and the MIT Kavli Institute. We are grateful for the support of the MIT Lincoln Laboratory's optical engineering staff for their help on this project.

REFERENCES

- [1] Fűrész, G. and The LLAMAS Collaboration, "Status update of llamas a wide field-of-view visible passband ifu for the 6.5m magellan telescopes," in [Proc. SPIE], **11447**(9) (2020).
- [2] Fűrész, G. and The LLAMAS Collaboration, "Optical design of fast a spectrograph camera and microlens-coupled ifu feed for the llamas instrument," in [Proc. SPIE], **11447**(111) (2020).
- [3] Nicodemus, F. E., "Reflectance nomenclature and directional reflectance and emissivity," *Appl. Opt.* **9**, 1474–1475 (Jun 1970).
- [4] Harvey, J. E. and Shack, R. V., "Aberrations of diffracted wave fields," Appl. Opt. 17, 3003–3009 (Sep 1978).